POLITECNICO DI TORINO

Master of Science's Degree in Biomedical Engineering

Politecnico di Torino

Master of Science's Degree Thesis

Redundant inertial sensor setup and constrained optimization for accurate golf putting orientation and trajectory estimation

Supervisors

Prof. Ing. Andrea CEREATTI

Dott. Ing. Marco CARUSO

Candidate

Niccolò TORTAROLO

December 2024

Abstract

The putting stroke in golf is a crucial component of the game, accounting for approximately 45% of the total strokes in a match. While professional players show 96% accuracy from 1 meter, performance drops dramatically to 65% from 2 meters. To maintain high accuracy, training is essential with precise trajectory feedback provided by specialized tools. Thus, the ability to maintain this level of precision lies in the accurate reconstruction of the putter's trajectory. Although different analysis systems exist, their main limitations are the impossibility of performing analysis in the open field and the high cost of equipment. In this context, inertial sensors (IMUs) which integrate an accelerometer and a gyroscope prove to be a feasible solution thanks to their relatively low cost and availability in real scenarios. The single IMU-based trajectory is typically estimated by double integrating the accelerometer signals after having removed the gravity vector projection obtained through a sensor-fusion filter for orientation computation. However, trajectories obtained using this non-optimized pipeline are not accurate enough due to the non-optimal setting of the filter parameter(s) and the rapid accumulation of measurement errors over time. In fact, position drifts can easily reach errors up to 0.5 m after a very few seconds. The goal of this thesis was the accurate reconstruction of the trajectory of the putter equipped with a redundant multi-IMU configuration through a constrained optimization framework. The accelerometer and gyroscope measurement errors were modeled as additive terms which are considered constant within the single trial duration. The objective function was designed to find the optimal values of the latter and the parameter values of the sensor fusion filter by minimizing the orientation of the IMUs rigidly attached to

the putter throughout the trial. The following constraints were also based on the specific knowledge of the task to avoid drifts in the velocity and position components of each IMU. During the static phase before and after the stroke in which the club was stationary: the norm of the accelerometer signal was set to be close to the gravity acceleration (condition 1), the mean of the acceleration and velocity was set to be null (conditions 2 and 3), and the maximum velocity value was set to be close to zero (condition 4). During the swing phase, the position of the putter head must remain non-negative, with a maximum height of 0.1 m. Due to the irregular shape of the putter, a rigid model was developed using the Denavit-Hartenberg convention to set the IMUs in a common and meaningful reference system. Model parameters were fitted through a static acquisition using the stereophotogrammetric system (SP). The putter was equipped with two IMUs (Xsens-MTw) placed on the shaft and head. Then, 22 stroke trials were recorded in a controlled environment. The putter reference orientation and trajectory were acquired by the SP. The accuracy during a putting stroke was evaluated in terms of root mean square error (RMSE) values for both position and orientation during the swing phase only. The optimal parameters allowed to achieve an average RMSE of 1.8 deg in orientation and 0.08 m in position, in comparison with the "non-optimized" where the errors were 1.7 deg in orientation and 0.15 m in position. These results seem to suggest the potentiality of a redundant IMU sensor configuration, marking a significant step towards integrating IMU technology into putting analysis.

Table of Contents

List of Tables

List of Figures

Acronyms

DH
Denavit-Hartenberg

DoF
Degree of Freedom

GCS
Global Coordinate System

IMU
Inertial Measurement Unit

LCS
Local Coordinate System

MEMS
Micro Electro-Mechanical System

PGA
Professional Golfer Association

QP
Quadratic Programming

RMSE
Root Mean Square Error

SFA
Sensor Fusion Algorithm

SP
Stereophotogrammetry

SQP

Sequential Quadratic Programming

Chapter 1

Introduction

1.1 Putting: Definition and Importance

Golf is widely recognized as one of the most difficult sports to learn, in which the primary challenge lies in coordinating body movements with the golf club to achieve the desired shot. Moreover, it is one of the most psychologically difficult sport, due to the game rules [1] [2] [3]. During a four-day tournament, players must maintain their concentration for approximately five hours a day, despite taking only about 65 shots per day, averaging one shot every five minutes. Consequently, the ability of golfer lies in avoiding mental distractions and maintaining focus on each individual shot. The variables are innumerable, and the margin of error is minimal. The equipment itself highlights the challenge: the goal is to hole in a golf ball with a diameter of about 0.04 m into a hole of 0.11m of diameter from hundreds of meters away using a club face with an average impact surface of 0.04 m by 0.07 m. This scenario emphasizes how crucial it is for golfers to achieve consistent and repeatable movements to perform reliable shots, coordinating body and club motions.

The golf game involves there being 18 holes on a course, each of which is characterized by an expected number of strokes to finish them, known as “par”. This can consist of a minimum of 3 strokes up to a maximum of 5 for professionals. According to the game’s rules, a player may have up to 14 different types of golf clubs at his disposal to achieve his goal, which consists in finishing all holes with

as few strokes as possible. Of the set of golf clubs available, 13 are used for the long and then the short game, during which the ball is expected to rise from the ground, and getting as close as possible to the hole by dropping the ball into the "Green". In particular, the latter corresponds to the area of the course where the hole is, where the grass is finer and the ground is more delicate, as it coincides with the place where the most accurate and important shot takes place. It is precisely here that the golfer relies on the fourteenth club: the "Putter" (Figure 1.1). In fact, of the 14 clubs previously mentioned, only the Putter is used at every hole, unless in exceptional cases. For this reason, it becomes evident that this type of shot, despite the fewer technical pitfalls compared with the others, is the most significant, being it the most frequently played.

Figure 1.1: Golf player putting in the green.

The Putter is characterized by certain technical features that define its functionality. The Grip, for instance, has a flat shape at the top, designed to provide a stable grip

and promote optimal hand alignment, helping to improve movement control. The Shaft, which is generally shorter than that of other clubs, is made of rigid materials, such as steel, to ensure precision and stability during stroke execution. The putter Head is engineered to offer balance and accuracy, with different configurations such as blade, mallet or semi-mallet to suit different playing styles. It also presents alignment lines that facilitate positioning relative to the ball and target. Focusing on the key geometric features, the Lie angle, usually between 70° and 74°, ensures optimal ground contact, while the Loft angle, of approximately 2° to 4°, is conceived to promote smooth ball rolling without initial bounce (Figure 1.2). Finally, the lower edge of the face, or edge, is often rounded to reduce friction with the turf, contributing to a smoother stroke.

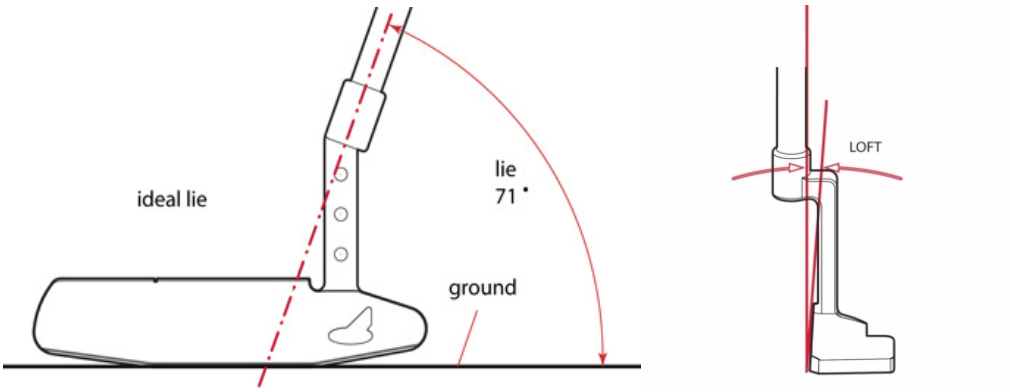

Figure 1.2: Lie and Loft angle of the putter [13].

Statistically, the most important shot in golf is the putting stroke [4], yet it is also the most underrated among amateur golfers. Putting typically accounts for approximately 40% of all strokes in a tournament for professional golfers and 50% for amateurs, underlining the importance of training to improve the reliability of the shot. The significance of this stroke lies in the famous motto among professional players: “Drive for show, putt for dough”, in which driving – the longest and most

thrilling shot – is more spectacular, instead of putting, which secures success and victory. While professional players show 96% accuracy from 1 meter, performance drops dramatically to 65% from 2 meters (Figure 1.3), demonstrating how sudden the rise in difficulty is as the distance increases [5].

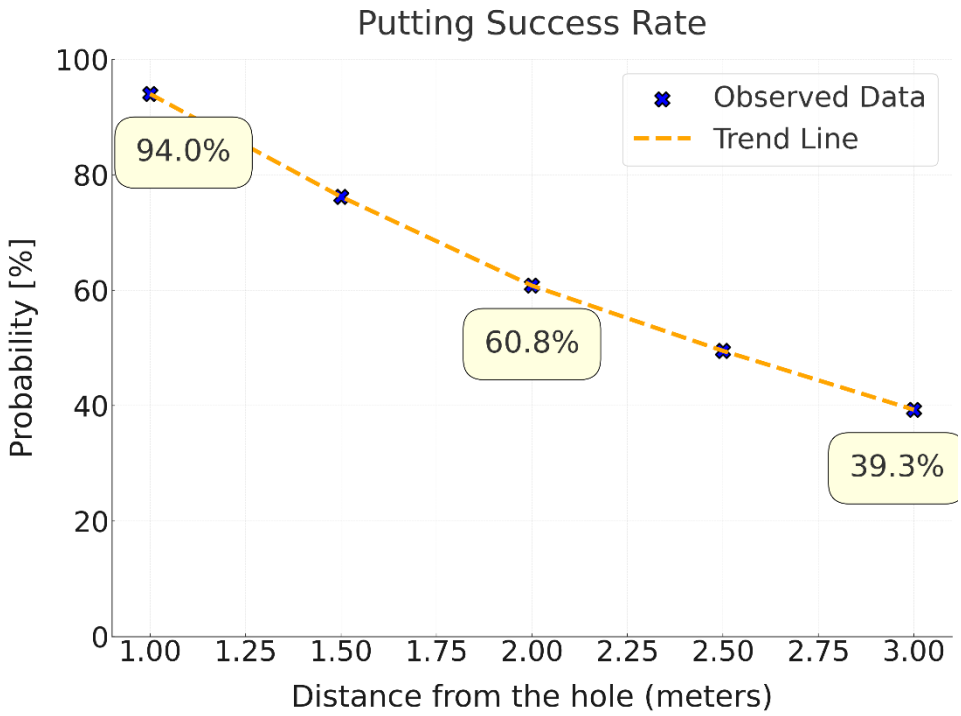

Figure 1.3: Percentage of successful putts on the PGA Tour (Professional Golfer Association).

This research, therefore, focuses on the study of the putting stroke. To evaluate this motion, two fundamental aspects must be considered:

- Biomechanics of the golfer: If the impact moment relies on the kinematics of the putt, then the latter depends on the golfer's biomechanics during the swing, creating an integrated system where the player and the club function as one.

- Kinematics of the putt: through this analysis, various parameters can be extracted, which are essential to determine whether the club's path complies with the standards needed for swing repeatability and, consequently, shot consistency. Differently from other clubs, the putting swing has a reduced speed, as it is executed at a close distance and requires great precision. The technical gesture in its phases is illustrated below in Figure 1.4.

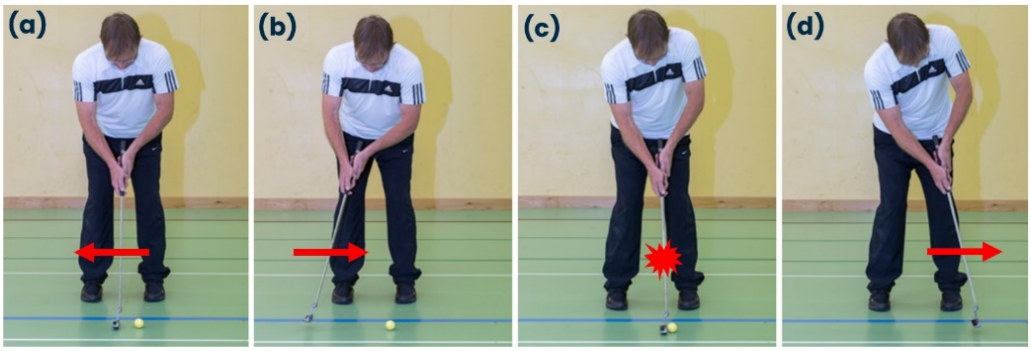

Figure 1.4: Putting swing phases comprehend Backswing (a), Downswing (b), Impact (c) and Follow-through (d) [18].

The precision in executing this stroke, therefore, depends on the golfer's ability to obtain a repeatable and consistent swing. As noted, the hole and ball dimensions are so small that every little variation in the swing could result in significant errors, which increase as the distance between the hole and ball increases.

As consequence of all these factors, effective putting training concentrates manly on developing:

- The techniques to strike the ball ensuring that it travels consistently in a straight line and reaches the intended distance.
- The ability to interpret the slopes and green conditions to take advantage on its contours effectively.

To execute an effective putt, the player must first analyse the Green to understand its contours and visualizes a feasible path for the ball to hole in. A strategic aiming point is then identified, and the distance to this target is evaluated. The objective is to direct the ball accurately toward the chosen point so that, through the impact with the putter and the subsequent interaction with the Green's surface, the ball follows the intended trajectory.

1.2 Market Overview

In literature and at the professional level, the inertial sensors developed are a tool mainly used to study the kinematics of the putter. The analysis of the golfer's biomechanics, on the other hand, is usually approached through the implementation of optical systems, sometimes assisted by ultrasonic sensors, for application simplicity. However, these systems present significant challenges: setup, calibration, acquisition and, above all, processing of data is extremely time-consuming, as many things must be set up and evaluated manually.

Up to now, the optical systems on the market evaluate the goodness of the shot by mainly analysing the kinematics of the club and the data at impact (e.g., SAM PuttLab [6] and Quintic Ball Roll [7]). The more sophisticated ones can even assess and evaluate the Green and the ball's trajectory during the shot, comparing the trajectory of the shot obtained against the one recommended and estimated by the sensor according to the hole reading, such as distances and slopes (e.g., Trackman 4 [8]). However, this instrumentation has limitations in use, as it is not portable and often requires a vast dedicated playing area.

Inertial sensors, on the other hand, have the convenience of being easily mounted on the putter. However, a detail not to be overlooked is the invasiveness of the

instrumentation that must be added to the club structure; indeed, it is necessary to use and position such instrumentation so that it does not affect the golfer's performance [12].

It is possible to note that the biomechanical part is neglected giving more relevance to the effectiveness of the shot, because there is no fixed rule for putting and every player can potentially develop his own technique aimed at improving the repeatability of the shot. Therefore, there is no standard on putting technique: some professional players, for instance, tend to have an "Address" and "Grip" that compensate for the peculiarities of their swing. It is precisely for this reason that the parameters (impact and swing metrics) identifying a correct execution are valued more importantly.

1.3 Literature Overview

In golf putt analysis, the increasing adoption of Inertial Measurement Unit (IMU) has emerged as a response to the significant limitations of optical tracking systems. These restrictions reside on the necessity of specialized facilities with a limited testing area, and all the challenges related to camera calibration, marker placement, and the expensive required equipment. Advancements in microelectronics have driven the development of IMU technology, allowing the possibility to integrate Micro Electro Mechanical System (MEMS) into compact units (Figure 1.5), such as accelerometers and gyroscopes. Thus, IMUs offer many advantages, including portability, compactness, lightweight and a wireless system.

Figure 1.5: Inertial Measurements Unit (Xsens-MTw).

Thanks to their compact size and affordability, IMUs can be effectively employed as wearable devices in open field scenarios beyond the controlled environment of a laboratory.

In this regard, many studies have been conducted to test the potential of IMUs in this area of analysis. First, it is important to evaluate where these can be placed on the putter, in order to prevent the club structure and thus the golfer's feel from being compromised. In this context, the study conducted by Kawano et al [12] stands out as an analysis of great interest, in which several configurations were tested to assess which had the least impact on the swing, providing an evaluation in terms of sensor placement and weight. This kind of technology is mainly implemented to perform swing phase analysis, neglecting trajectory and focusing on obtaining interesting swing phase and impact parameters [14] [15], through sensor calibration, signal filtering and zero-crossing methods. This is mainly caused by the limitations of IMUs, which lie precisely in the recording of measurement errors and consequently lead to drift errors in position integration. Several studies have attempted to estimate the complete trajectory of the golf club, but with many difficulties, particularly

concerning the recording duration. Most of these have exploited the Kalman filter to trace the sensors' orientation and then, once the bias was removed from the sensors, estimate the position, either from the grip [17] or from the head [16].

Consequently, during the analysis of the putting stroke, IMUs enable the assessment of kinematics parameters [9], including the club's path and orientation. Although their accuracy may not match that of optical system as the Stereophotogrammetric (SP), they could offer a practical alternative for real-time feedback and training applications, as demonstrated in previous studies: these researches, where a putter with integrated IMU sensor was designed [10] [11], demonstrated errors of the order of a few centimeters in the data estimation phase.

Thus, the use of IMU has emerged as a possible solution in putting analysis. IMUs, which can capture crucial kinematic data, provide direct insights into the putter's motion and the golfer's technique, without relying on any external acquisition system, allowing the possibility of data collection in various environments and real-time analysis.

Therefore, the main challenge of this work consists in overcoming the limitations encountered in the literature for the analysis of putting, where the usage of low-cost inertial sensors implies registration quality problems, especially for long recordings. Indeed, it is known from the literature [28] that errors and measurement inaccuracies induce errors in terms of drift for position estimation, precisely because these errors, when integrated, tend to progressively accumulate over time. As a result, part of the estimate precision and accuracy is lost after a few seconds: indeed, as illustrated later, the unconstrained standard methods can lead to meters of drift, even on paths of a few centimeters.

1.4 Aim of the Thesis

This study aims at addressing the challenge of developing a putting analysis system, through the implementation of inertial sensors, that overcomes the limits of existing technologies, in terms of cost and usage in the open field.

The primary focus resided in the development of the proposed method, which concentrates on the estimation of putting stroke kinematics by relying on a small number of IMUs in a redundant configuration.

The choice of the number and placement of sensors needed was made taking into consideration the limits of the devices, where sensors alone are unreliable because they are corrupted by too many errors. In this sense, after the evaluation of several configurations performed in the literature, this study proposes a redundant configuration of IMUs to mitigate the errors recorded by the individuals, assuming that these are different from each other. More particularly, the gyroscopes' errors are un-related [28], whereas those of the accelerometer are mainly related to calibration residuals, which result in further errors in the subsequent steps, where orientation must be estimated in order to remove gravity.

Consequently, a redundant configuration was studied to enhance accuracy and minimize errors, where two inertial sensors were placed in the Shaft e Head of the putter. This configuration enables the extraction of swing parameters from the IMUs placed on the putter, allowing for an estimation of the putter's trajectory without affecting the swing feeling.

The challenge of this thesis resides in the fact that two IMUs alone do not provide sufficient data to derive complete and accurate putter trajectory due to the lack of information and the limits of this technology, as the trajectories estimated by these

IMUs are affected by errors. Therefore, to overcome these difficulties, an optimised approach and a model of the putter must be introduced to address these gaps.

1.5 Thesis Outline

The thesis is structured as follows:

Chapter 2 presents an overview on IMUs and orientation estimation techniques, utilizing Sensor Fusion Algorithm (SFA) in both standard and proposed pipelines.

In **Chapter 3**, the employed methods are elucidated. This section explores the interaction between the developed Denavit-Hartenberg (DH) model and IMU sensor data, focusing on the combination of these components within an optimization framework aimed at the reconstructed putter kinematics.

Chapter 4 details the experimental session and a comprehensive description of the data acquisition process.

In **Chapter 5**, the results obtained with the implemented optimization framework are reported, presenting Root Mean Square Error (RMSE) values in terms of orientation and position to evaluate the accuracy.

In **Chapter 6**, a critical evaluation of the results presented in Chapter 5 is carried out.

In **Chapter 7**, a summary of the main findings is presented, laying the foundation for future research.

Chapter 2

State of the art

2.1 Inertial Measurement Units

IMU sensors rely on the combination of tri-axis accelerometers and gyroscope, which are orthogonally installed, recording the combined linear and gravitational accelerations and the angular velocity in relation to their Local Coordinate System (LCS) [20]. It is possible to acquire a complete estimation of the LCS orientation relative to the Global Coordinate System (GCS) through the application of SFAs, which accurately combine the sensors' signals by evaluating the orientation related to the local direction of the gravity vector [21].

As disclosed in Equation 2.1, accelerometers record the "specific force" ($\boldsymbol{a}$), representing the vector difference between the body's acceleration ($\boldsymbol{a_{body}}$) and the gravity acceleration ($\boldsymbol{g}$). All quantities are expressed within the LCS of the sensor, with the following output:

$$\boldsymbol{a} = (\boldsymbol{a_{body}} - \boldsymbol{g}) \tag{2.1}$$

During the free-fall of the sensor, the $\boldsymbol{a_{body}}$ term is equal to $\boldsymbol{g}$ and consequently, the accelerometer output results zero. On the other hand, when the device is stationary and unaltered by external forces or acceleration, the $\boldsymbol{a_{body}}$ contribution is null, allowing the accelerometer to sense only the gravitational acceleration, in the same manner as an inclinometer. Thus, when the sensor is moving, it becomes challenging to accurately estimate the inclination of the accelerometer, since the

body's acceleration overlaps with the gravitational component. To this end, it is possible to distinguish these contributions and obtain a reliable estimate with the integration of additional information.

This additional information is generally modelled as error components in the accelerometer signal. This provides the basis for studies that rely on models to separate the different components, for instance the bias and its fluctuations or the scaling matrix [22] [23] [24] [25].

Then, a simplified model was carried out, as shown in Equation 2.2, evaluating the needs and circumstances of the situation under analysis, as it will be further discussed in the next sections. For this reason, the different error components were merged into a single one, the accelerometer bias $\boldsymbol{b_a}$, which is considered constant during the trial, thus simplifying the computational load of the proposed method.

$$\boldsymbol{a} = \left(\boldsymbol{a_{body}} - \boldsymbol{g}\right) + \boldsymbol{b_a} \tag{2.2}$$

Just as for the accelerometer, the gyroscope also requires modelling the sensor output (Equation 2.3). Gyroscopes detect angular velocity along their axes. Various models for gyroscope output exist in the literature, primarily differing in the complexity of the different error contribution [22,23,25,26,27,28,29,30,31]. As performed before for the accelerometer, a simplified gyroscope output model is proposed:

$$\boldsymbol{\omega} = \boldsymbol{\omega_{body}} + \boldsymbol{b_\omega} \tag{2.3}$$

with $\boldsymbol{b_g}$ that representing the gyroscope bias, considered constant within the single trial duration. Moreover, $\boldsymbol{b_\omega}$ stands out as the most significant term of impact on the orientation estimation. Indeed, the integration of the angular velocity affected by errors introduces drift on the estimated orientation, which is crucial to correctly

remove the gravity vector from the accelerometer signal to avoid displacement drift thought the double integration, necessary to obtain the position [19].

2.2 Orientation Estimation based on a Sensor Fusion Approach

By relying on SFA, it is possible to estimate the orientation combining the characteristics of the individual IMU sensors. This method exploits the integration of accelerometer and gyroscope measurements, allowing to obtain an estimate of the three-dimensional orientation of an IMU and, more generally, of the rigid body to which it is attached. To determine the absolute orientation of the IMU in three-dimensional space, it is necessary to define the rotation between its LCS and the GCS. This is essential to eliminate the gravitational contribution from the accelerometer signals, enabling the integration of linear velocity and displacement. In the literature, the SFAs presented are numerous, many of which can be classified into the complementary or Kalman filter families, differing mainly in orientation parametrization (e.g., orientation matrices, quaternions, Euler angles), variants of the Kalman filter (e.g., linear, extended, etc.) and in the fusion strategies implemented (based on optimization or algebraic approaches). One of the most used filters is the Madgwick one [32], a complementary filter that relies on quaternions to estimate the orientation. This filter is appreciated for its application simplicity and involves a low computational cost since it requires the calibration of a single parameter $\boldsymbol{\beta}$.

The essential method to obtain the orientation from the IMU data consists initially in integrating the angular velocity, then refined with the accelerometer measurements. Consequently, the accelerometer data are employed in an optimized

gradient descent algorithm that, through the quaternion derivative, allows the calculation of the direction of the gyroscope measurement error. The parameter $\boldsymbol{\beta}$ plays a crucial role, being related to the zero mean of the gyroscope measurement errors; a higher value of $\boldsymbol{\beta}$ increases the importance of the signals coming from the accelerometer. The accuracy of IMU orientation, determined through various SFAs, has been the focus of numerous studies in recent years. However, the results obtained have often been conflicting [20,33,34,35,36,37,38,39]. Indeed, the difficulty in achieving consistent and generalizable results lies in the necessity to calibrate, for each SFA, the parameters that regulate the sensor fusion process.

A critical aspect is represented by the choice of parameter values, which is influenced by both intrinsic factors (e.g., intensity of sensor noise) and external factors (e.g., amplitude of the motion) [40]. Research proves that optimal parameter selection can significantly improve the accuracy of the estimated orientation, but finding suitable values is not simple. Indeed, there is no standardized configuration procedure that can be universally applied, which further complicates the process of generalizing the results. A possible approach could be to identify optimal parameter values minimizing the error between the estimated and reference orientations by analysing specific recordings. Additionally, it has been highlighted how each fusion algorithm tends to achieve optimal performances only within a narrow range of parameters [41]. In this context, variations in the experimental conditions could lead to significant errors if the calibrated parameters for different scenarios are maintained. This phenomenon demonstrates the necessity for a specific tuning of the parameters based on the experimental conditions [37,42], in order to ensure adequate performances for each SFA.

2.3 General Description of the Analysed Situation

The scenario under analysis evaluates the club's trajectory during a putting stroke, equipped with two inertial sensors placed in strategic positions: Shaft and Head of the golf club. At first, it is essential to reconstruct a detailed model of the golf club to be able to establish the initial conditions of the sensors mounted on it. Since the golf club is considered a rigid body, the initial positions of the sensors remain constant with each other throughout the trial. Due to the complex geometry of the putter, highlighted in Figure 2.1, we adopted an initial optimisation framework to define the structural parameters of the putter. This allowed us to establish the orientation matrices that locate and orient the sensors mounted on the putter.

To obtain an accurate estimation of the trajectory, an additional optimisation framework was required. This second approach is fundamental to clean the sensor signals of any errors and, through the SFA, ensure consistent orientation estimation. This step is crucial to avoid error drift in the subsequent integration steps required to determine the position of the putter. This methodological approach aims to minimise error accumulation and ensure measurement accuracy during the kinematic analysis of the stroke.

Figure 2.1: Putter Odyssey White Steel 2-Ball Blade.

2.3.1 Standard Pipeline

The use of SFAs allows the orientation of the sensors to be accurately estimated, making it possible to analyse the putting stroke even in the open field. Accurate estimation of the orientation of the sensors is the first step to an effective kinematic analysis of the shot. However, for this to be possible, it is necessary to align the LCSs of each sensor with respect to the GCS, taking into consideration the specific placement of each sensor in relation to the different sections of the golf club. Consequently, in order to obtain an accurate estimate of the kinematics of the putter,

it is crucial to establish and maintain a rigid and time-invariant relationship between the various segments of the club, which behaves as a rigid body divided into several segments connected by joints with zero degrees of freedom. A further challenge arises in estimating the kinematics without the use of a magnetometer, which limits the information on the relative orientation between IMUs in the horizontal plane. Without the direction of the Earth's magnetic field, it is not possible to define a single horizontal axis in the GCS, which has the vertical axis aligned with the gravity vector and one of the horizontal axes oriented in the direction of the Earth's magnetic field projected onto the horizontal plane. In the absence of magnetometric data, the alignment is achieved by having the x-axis of the GCS coincide with the x-axis of the single IMU.

As a basic approach (Figure 2.2), a standard method using Madgwick's filter was adopted to estimate the orientation of the sensors [32]. Subsequently, by removing the gravitational component and integrating the signals, the position of the individual sensor in space during the trial can be derived. For this procedure, the parameter $\boldsymbol{\beta}$ (constant for both sensors) and the bias of the gyroscope $\boldsymbol{b_{\omega}}$, obtained from a recording made under static conditions, were predetermined for each sensor. Additionally, the putter model proves to be useful in developing a more reliable model of the club's rigid structure, facilitating calculations for sensor fusion.

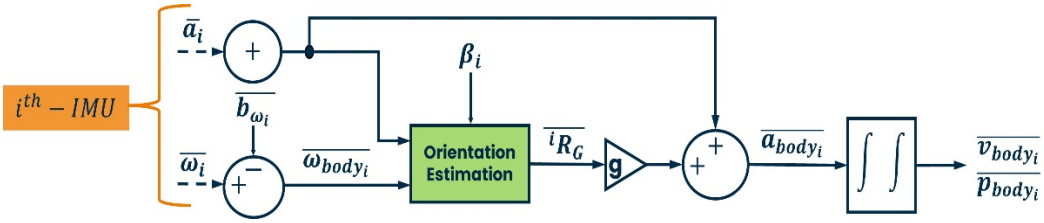

Figure 2.2: Schematization of the standard pipeline ($i^{th} - sensors$).

This method, however, has limitations. The absence of specific constraints leads to measurement errors due to inaccurate estimates of $\boldsymbol{b_\omega}$ and the lack of a corrective for possible accelerometer bias errors $\boldsymbol{b_a}$. These errors, when integrated, tend to accumulate exponentially, compromising the accuracy of the estimate. In addition, the choice of a constant $\boldsymbol{\beta}$ parameter for all sensors is inefficient, as each sensor would require a specific $\boldsymbol{\beta}$ value to guarantee greater accuracy, adapting the solution to the characteristics of each device.

2.3.2 Proposed Pipeline

The estimation of the orientation of each sensor through Madgwick's filter, although useful, may not guarantee sufficient accuracy for a correct analysis of the displacement and, consequently, the kinematics of the putter. In this context, it becomes crucial to introduce an optimisation framework to identify the optimal combination of key SFA parameters, such as $\boldsymbol{\beta}$ and the modelled error terms for the accelerometer and gyroscope, respectively $\boldsymbol{b_a}$ and $\boldsymbol{b_\omega}$. This approach is aimed at improving the performance of the SFA itself, enabling a more accurate estimation of the club's displacement in space. The aim of this study is, therefore, to improve the performance of the inertial sensors for kinematic analysis of putting directly on playing fields, by exploiting a redundant system of IMUs and an optimisation framework. This approach addresses the difficulties arising from the lack of complete data to derive the necessary kinematic equations.

Chapter 3

Methods

3.1 Putter Model

For the reconstruction of the golf club trajectory, it was essential to use a model implemented through MATLAB R2022b (The MathWorks Inc, MA, USA), to characterize the analysed putter. At this early stage, the optimisation of the structural parameters of the putter was essential to accurately define the putter model following the DH convention. This enabled to estimate precisely the sensor orientations based on their specific positioning on the putter.

3.1.1 The Denavit-Hartenbeg Convention

In order to accurately model the golf club, it was necessary to adopt a convention to define a rigid kinematic chain of the putter. For this purpose, the DH convention was applied, which is based on the construction of a kinematic chain using "links" to connect the "joints" to each other, as presented in Figure 3.1 [43]. This methodology is fundamental for establishing the orientation and position of the links within the structure. The transformation matrix $\boldsymbol{A_i^{i-1}}$ of the i^{th} link with respect to the previous $(i-1)^{th}$ is a $4x4$ matrix, which integrates both the $3x3$ orientation matrix and the $1x3$ translation vector. The parameters defining the transformation matrix (Equation 3.1) are:

- $\boldsymbol{a_i}$ distance between O_i and $O_{i'}$;

- $\boldsymbol{d_i}$ coordinate of $O_{i'}$ along z_{i-1} ;
- $\boldsymbol{\alpha_i}$ angle between axes z_{i-1} and z_i about axis x_i to be take positive when rotation is made counter-clockwise;
- $\boldsymbol{\theta_i}$ angle between axes x_{i-1} and x_i about axis z_{i-1} to be take positive when rotation is made counter-clockwise.

$$A_i^{i-1} = \begin{bmatrix} cos(\boldsymbol{\theta_i}) & -sin(\boldsymbol{\theta_i})\cos(\boldsymbol{\alpha_i}) & sin(\boldsymbol{\theta_i})\sin(\boldsymbol{\alpha_i}) & \boldsymbol{a_i}\cos(\boldsymbol{\theta_i}) \\ sin(\boldsymbol{\theta_i}) & cos(\boldsymbol{\theta_i})\cos(\boldsymbol{\alpha_i}) & -cos(\boldsymbol{\theta_i})\sin(\boldsymbol{\alpha_i}) & \boldsymbol{a_i}\sin(\boldsymbol{\theta_i}) \\ 0 & sin(\boldsymbol{\alpha_i}) & cos(\boldsymbol{\alpha_i}) & \boldsymbol{d_i} \\ 0 & 0 & 0 & 1 \end{bmatrix} \quad (3.1)$$

According to the DH convention, each joint is modelled with a single Degree of Freedom (DoF), called $\boldsymbol{\varphi}$, which describes the rotation of the joint. Furthermore, as revolute joints are used, while the first three parameters are constant and depend on the geometric configuration of the links between two consecutive joints, $\boldsymbol{\theta_i}$ is typically time-varying to adapt to different chain configurations. However, in the specific case of the putter, which is a rigid body, $\boldsymbol{\theta_i}$ is also kept constant to preserve the integrity of the kinematic chain, being uniquely defined by the geometry of the model.

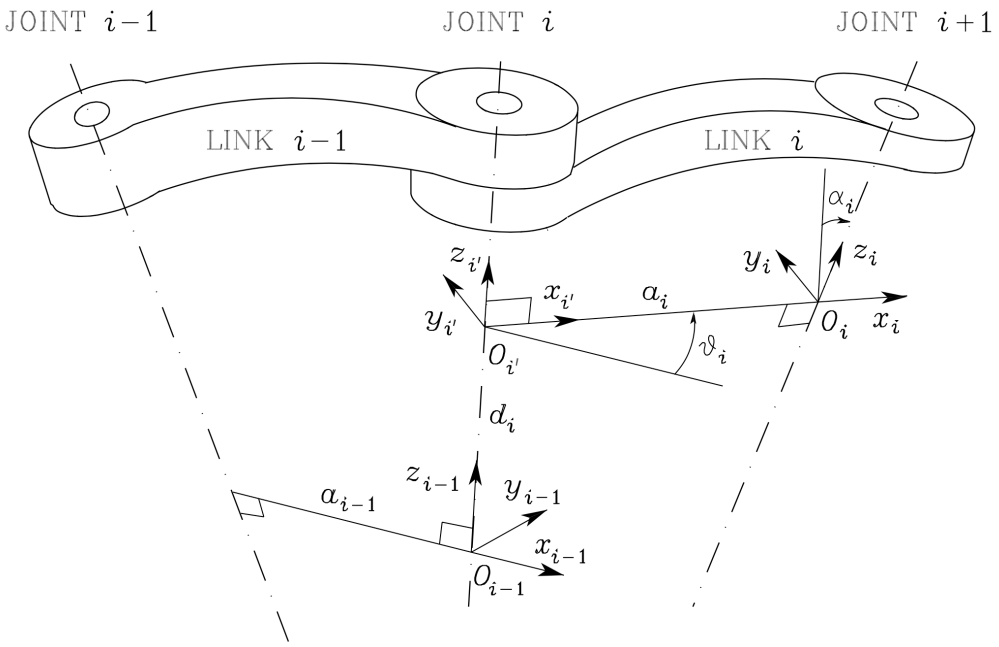

Figure 3. 1: Denavit-Hartenberg convention [43].

3.1.2 Developed Putter Model

In order to model the putter equipped with two IMU sensors (Shaft and Head), a kinematic chain connecting the sensors was created respecting the geometry of the rigid body under analysis. For this structure, 10 links and 11 joints were adopted (Figure 3.2). Since the putter is a rigid body, only the first three joints, starting with the top of the club, were defined as rotary (three DoFs: φ_1, φ_2, φ_3), thus incorporating all possible movements that can be executed during a stroke. Consequently, the downstream joints, and thus also the sensors, will move in response to these movements. The model of the putter is therefore characterised by a series of 14 parameters describing the measurements of its geometry (Table 3.1).

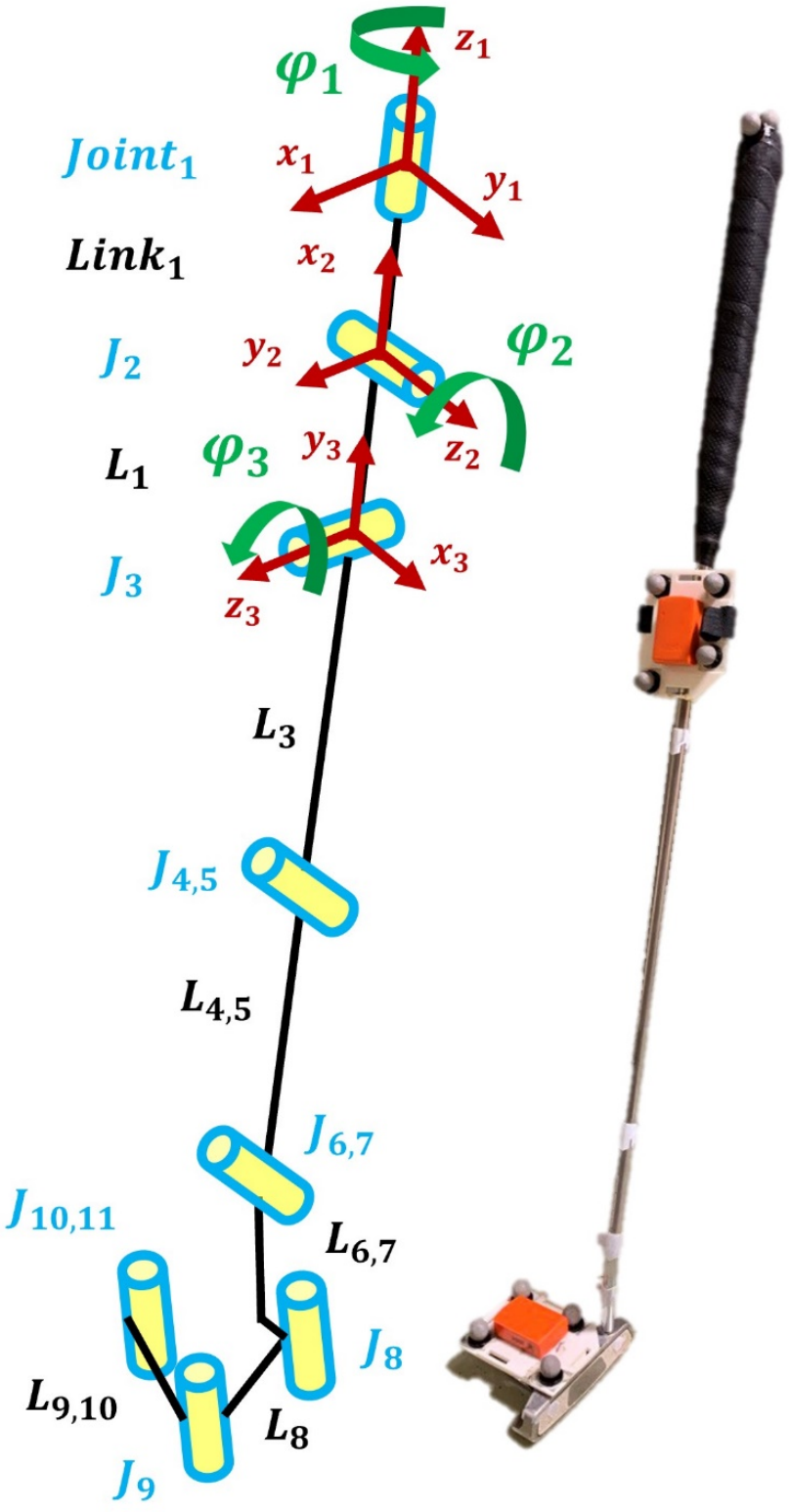

Figure 3. 2: Denavit-Hartenberg model of the putter

Link	$\boldsymbol{\theta_i}$	$\boldsymbol{d_i}$	$\boldsymbol{a_i}$	$\boldsymbol{\alpha_i}$
1	$\varphi_1 + \pi/2$	0	0	$\pi/2$
2	$\varphi_2 + \pi/2$	0	0	$\pi/2$
3	$\varphi_3 + \pi/2$	0	0	0
4	0	$-l_{gr}$	0	0
5	$\pi/2$	$-l_{sh}$	0	α_5
6	$-\pi/2$	0	0	$-\alpha_6$
7	0	$-d_7$	a_7	0
8	0	0	a_8	0
9	π	d_9	a_9	0
10	$\pi/2$	0	a_{10}	0

Table 3.1: Parameters of the putter model

3.1.3 Optimised Putter Model

To ensure greater accuracy in the subsequent calculations and to avoid errors due to incorrect manual measurements of the putter's characteristic parameters, it was necessary to implement a preliminary optimisation of the club geometry estimation, given the complexity of its structure (Figure 3.2).

To this end, an objective function was implemented to improve the accuracy in estimating the characteristic parameters of the putter geometry compared to manual measurement. These parameters are crucial for precisely defining the DH model and correctly determining the orientation of the IMUs placed on the club. Out of the 14 characteristic parameters of the putter, 3 were known, while the other 11 were optimised.

The optimisation was carried out by means of a static acquisition with 16 markers using a SP system. The objective function, in this case, minimises the distance between the estimated points of the model and those detected by the SP system, ensuring a better correspondence between the estimated and actual geometry. As a results of this approach, the residual obtained equals to 2.55×10^{-6}.

3.2 IMU-Based Information

Thanks to the accelerometers and gyroscopes, it is possible to monitor the linear acceleration and angular velocity of the individual sensors during the entire trial. This data is crucial for obtaining an accurate estimate of the putter trajectory via the SFA. For this reason, the importance of the integration of the optimisation framework will be discussed in more detail in the following paragraphs, both to make the best use of the SFA and to correct any errors in the data collected by the IMUs during the trials, as the integration of such data tends to generate an increasing cumulative error.

3.2.1 Orientation Estimation

The estimation of the orientation of the two IMUs is obtained through the SFA method proposed by Madgwick in [32], which relies on a complementary quaternion-based orientation filter. This approach was adopted for its implementation simplicity, as it is based on the setting of a single parameter, $\boldsymbol{\beta}$. As a result, the computational load is reduced, a prerequisite for the subsequent optimisation steps.

To determine the orientation using IMU data, the first phase concerns the integration of the angular velocity provided by the gyroscope. However, as this process is subject to cumulative errors, the estimated orientation is corrected using the accelerometer readings. The correction is made using an optimised gradient-descent algorithm, which utilises the accelerometer data to calculate the direction of the gyroscope measurement error as a quaternion derivative. In this regard, it is crucial to correctly set $\boldsymbol{\beta}$, the primary parameter of the filter that governs its behaviour. This value represents the zero mean of the gyroscope's measurement errors; therefore, when it assumes values greater than zero, it tends to give greater importance to the accelerometer's contribution. For this study, the chosen value for $\boldsymbol{\beta}$ was set at 0.001.

The algorithm follows an iterative cycle in which, at each time step, the orientation is updated based on that calculated at the previous step. To start this process correctly, it is essential to select a suitable initial quaternion. It is reasonably assumed that, at the beginning, the rigid body connected to the IMUs is in a stationary condition, before any motion begins. This assumption permits to adopt an initialisation method that uses only the accelerometer data and initially avoids considering the gyroscope data. Subsequently, the orientation was estimated by combining the information provided by the accelerometer and gyroscope (Figure 3.3). To improve the accuracy of the calculations, the gyroscope offset was reduced by averaging the angular velocity values recorded during static conditions.

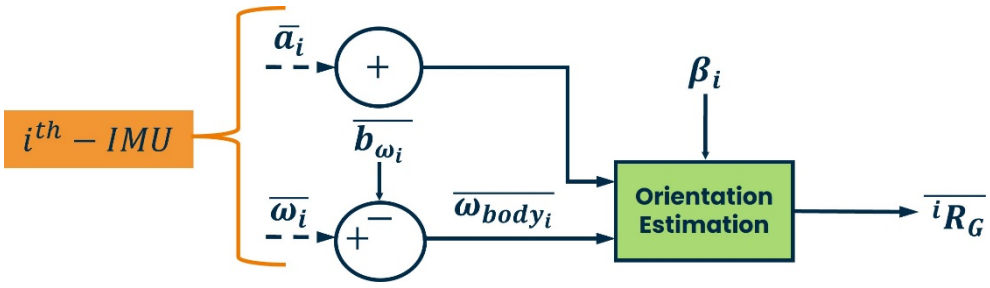

Figure 3. 3: Overview of the orientation estimation ($i^{th} - sensors$).

3.3 Definition of the Optimisation Framework

In this section, the optimisation framework will be examined, focusing on the optimisation algorithm used and, on the optimisation implemented. The purpose of this approach is to obtain a more precise estimate of the essential SFA parameters, necessary for an accurate reconstruction of the trajectory. In addition, a constraint function will be illustrated, designed to impose conditions during optimisation that favour an estimation of the trajectory that is closer to reality.

3.3.1 The Sequential Quadratic Programming Algorithm

The optimisation framework implemented relies on the Sequential Quadratic Programming (SQP) algorithm, an iterative method particularly suited for constrained non-linear optimisation. This approach involves solving a series of optimisation subproblems using a quadratic model of the objective function and a linearisation of constraints. The process is based on a quadratic approximation of the Lagrangian function, formulated as a Quadratic Programming (QP) problem. The solution of each subproblem provides a new iteration point, progressively improving the optimisation. Therefore, the SQP method can be considered a quasi-

Newton method that exploits the properties of QP subproblems to converge to an optimal solution, as illustrated in Figure 3.4.

Consider a general non-linear programming problem formulated as follows:

$$min_x\ f(x)$$

$$subject\ to\ \ h(x) \geq 0,\ \ g(x) = 0$$

The Lagrangian associated with the problem is given by:

$$\mathcal{L}(x, \lambda, \sigma) = f(x) - \lambda h(x) - \sigma g(x) \qquad (3.2)$$

where $\boldsymbol{\lambda}$ and $\boldsymbol{\sigma}$ are the Lagrange multipliers. To find a solution $\boldsymbol{\nabla \mathcal{L}(x, \lambda, \sigma) = 0}$ that satisfies the optimal conditions, the SQP algorithm computes a search direction $\boldsymbol{d_k}$ from a current iteration $(\boldsymbol{x_k, \lambda_k, \sigma_k})$, solving the QP subproblem. In the absence of constraints, the algorithm reduces to Newton's method, which goal is to find a point at which the target gradient equals to zero [44]. The implementation of the SQP algorithm involves the following main steps [45]:

- Updating the Hexian matrix.
- Solving the quadratic programming subproblem to obtain the search direction.
- Initialisation of the optimisation parameters.
- Line search and evaluation of the merit function to ensure convergence.

Consequently, the algorithm requires well-defined initial conditions and a clear objective function to be minimised in order to work properly.

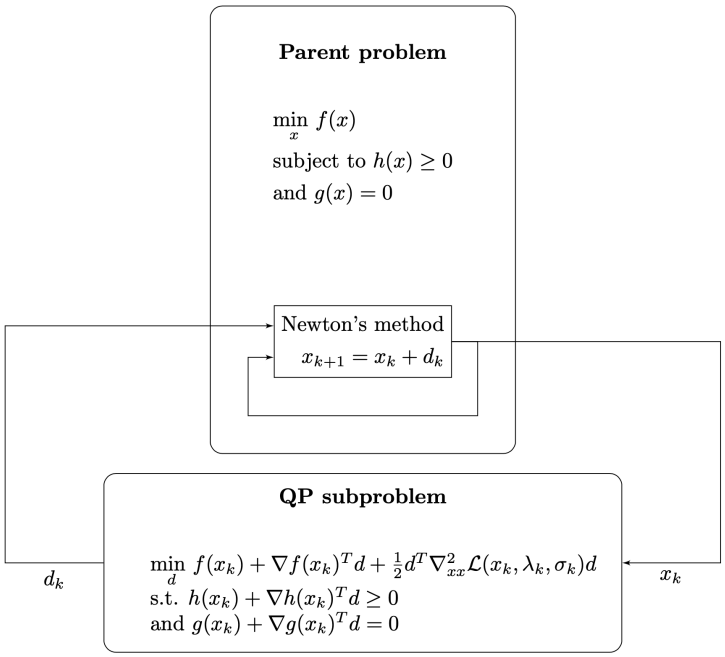

Figure 3. 4: General scheme illustrating the basic SQP algorithm [33]. The terms f(x), h(x), and g(x) are each potentially non linear; x is potentially a vector of many variables for the optimization, in which case h(x) and g(x) are systems. ∇^2_{xx} denotes the Hessian matrix.

3.3.2 Objective Function

The implemented framework (Figure 3.5) is significantly complex, as it requires the optimisation of multiple parameters to minimise the objective function. The variables to be optimised for each IMU sensor are:

- $\boldsymbol{\beta}$ parameter of the Madgwick filter
- Residual Gyroscope bias $\boldsymbol{b_\omega}$ along the three axes
- Accelerometer bias $\boldsymbol{b_a}$ along the three axes

With two sensors placed on the putter, the total number of parameters to be optimised is 14. For each parameter, an upper and lower limit was defined according to the situation analysed. In addition, $\boldsymbol{\beta}$ and $\boldsymbol{b_a}$ were initialised to null

values; instead, $\boldsymbol{b_\omega}$ was initialised equal to the bias value recorded under static conditions for both sensors. In addition, the putter model was exploited to orient the rotation matrix with respect to the putter reference system. Consequently, the objective function $\boldsymbol{f_{obj}}$ at this phase aims to minimise the relative difference in orientation between the two sensors throughout the trial [48]. Specifically, once the optimised bias was removed from the accelerometer and gyroscope signals, and the Madgwick filter with the optimised $\boldsymbol{\beta}$ value was applied, it was possible to obtain the accurate orientation of each sensor. Thanks to the optimised parameters, it was then possible to repeat the previously defined steps to estimate the orientation precisely and, consequently, reconstruct the trajectory of the putter.

$$\min f_{obj}\left(\overline{\boldsymbol{b_{a_i}}}, \overline{\boldsymbol{b_{\omega_i}}}, \boldsymbol{\beta_i}\right) = \begin{cases} \left(\overline{{}^{Shaft}\boldsymbol{R_P}}\right)^T * \overline{{}^{Head}\boldsymbol{R_P}} \\ \forall\, i = \{1,2\} \end{cases}$$

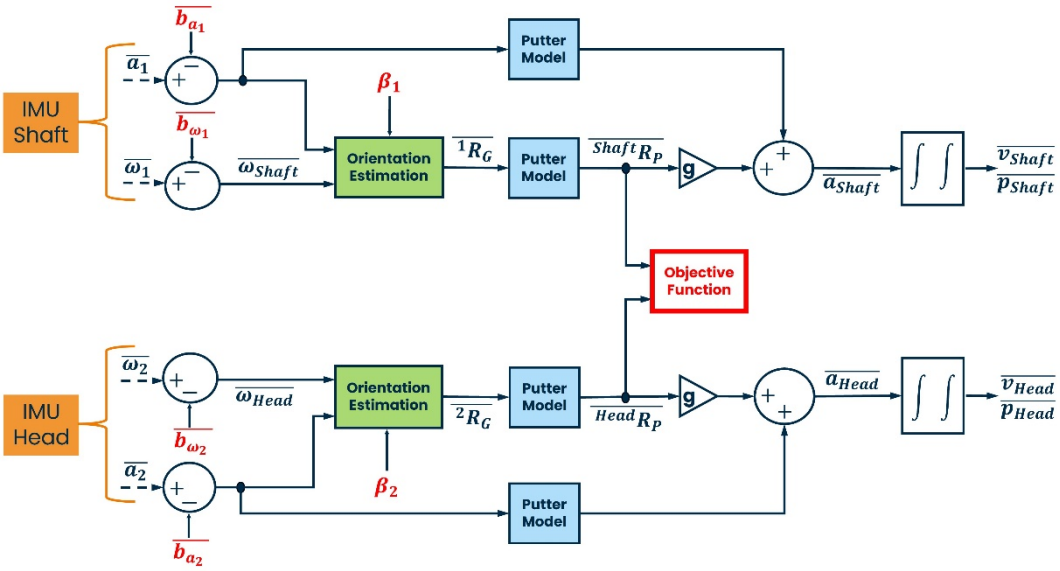

Figure 3. 5: Overview of the optimization framework ($i^{th} - sensor$).

Before reaching the final version of the framework, various combinations of the parameters to be optimised were tested to find the optimal configuration. The tested

partial combinations and their improvements will be discussed in detail in Section 5.

3.3.3 Constraint Function

As will be evident in Section 5, in which the results obtained will be discussed, the use of the objective function alone for the optimisation is not sufficient to obtain an accurate estimate of the putter trajectory, since even a minimal residual error in the data recorded by the IMU, once integrated, leads to a progressive accumulation of error in the calculated displacement. To avoid drift errors, it was therefore necessary to introduce a non-linear constraint function. The latter, during optimisation, evaluates the acceleration, velocity and position vectors, verifying that certain conditions are satisfied at specific stages of the swing. The constraints imposed during the trials (Figure 3.6), designed to achieve more valid parameter optimisation, are described below.

During static phases before and after the stroke:

- Inequality constraint: norm of the accelerometer signal between $9.80 - 9.82\ m/s^2$
- Equality constraint: average acceleration equal to a $0\ m/s^2$
- Equality constraint: average velocity equal to a $0\ m/s$
- Inequality constraint: maximum of the velocity magnitude between $0 - 0.005\ m/s$

During the entire swing phase:

- Inequality constraint: position of the putter head along the axis perpendicular to the ground between $0 - 0.1\ m$

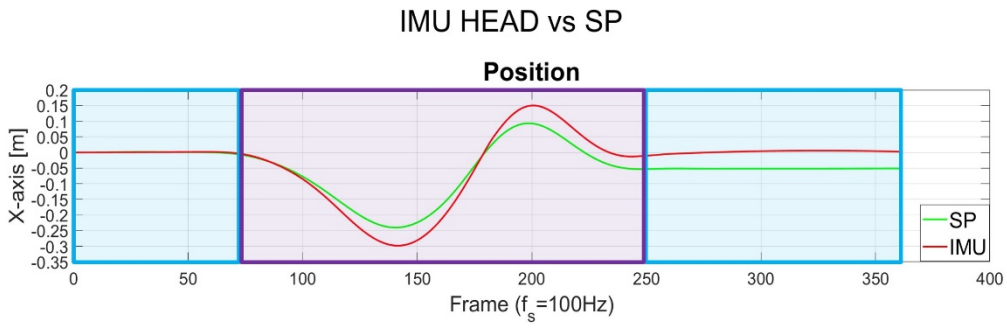

$$\text{Constraint Function} = \begin{cases} \textit{Static phases} \begin{cases} 9{,}80\ m/s^2 < norm(\overline{\boldsymbol{a}_{1,2}}) < 9{,}82\ m/s^2 \\ mean(\overline{\boldsymbol{a}_{\boldsymbol{Shaft,Head}}}) = 0\ m/s^2 \\ mean(\overline{\boldsymbol{v}_{\boldsymbol{Shaft,Head}}}) = 0\ m/s \\ 0\ m/s < \max(abs(\overline{\boldsymbol{v}_{\boldsymbol{Shaft,Head}}})) < 0{,}005\ m/s \end{cases} \\ \textit{Swing phase} \begin{cases} 0 < \overline{\boldsymbol{p}_{\boldsymbol{Head_z}}} < 0{,}1\ m \end{cases} \end{cases}$$

Figure 3. 6: Constraint Function and an example of the Head position along the x-axes

3.4 Estimated Orientation and Trajectory

Following the optimisation, it is possible to proceed with the evaluation of the putter trajectory. With the optimised parameters, an accurate estimation of the orientation during the entire trial is obtained. This allows to remove the gravitational component from the accelerometer signal of each sensor, based on its orientation, and subsequently integrate the signal to calculate the velocity and position of the IMUs, thus determining the trajectory of the club.

To verify the accuracy of the calculated data, the results were compared with those obtained through the SP marker system equipped on the putter. For a quantitative evaluation of the estimation, the RMSE was calculated, which measures the differences between the results derived from the IMUs and those provided by the SP.

As will be discussed in Section 5, the RMSE calculation was implemented to compare orientation and position for each IMU, ensuring a comprehensive analysis of the differences

Chapter 4

Experimental procedure

4.1 Setup

This experimental study was carried out within the PolitoBIOMed Lab, a laboratory of the Polytechnic of Turin equipped with advanced instrumentation for the study and analysis of motion, as shown in Figure 4.1. Two main systems were used for data acquisition:

1) Vicon-Vero SP system as the gold standard, consisting of:
    - 12 Vicon infrared cameras to reduce artefacts caused by natural light, ensuring accurate tracking;
    - 3 RGB cameras for video recording of the experiments;
    - An active wand was used to calibrate the system, using known geometric marker configurations (Figure 4.1);
    - 16 passive markers, coated with retro-reflective material, were placed on the putter, as shown in Figure 4.2;
    - Nexus software (v. 2.11) was utilized for extracting files.
2) Xsens-MTw IMU-based system: two IMUs were fixed on specific putter segments (Shaft and Head) for motion tracking, operating at a sampling rate of 100 Hz. Each IMU within the system includes (Figure 4.3):
    - 3D accelerometer with a selectable full-scale range up to $\pm 16g$;
    - 3D gyroscope with a full-scale range selectable up to $\pm 2000\ °/s$.

Figure 4.1: PolitoBIOMed Lab with Vicon-Vero System and Active Wand.

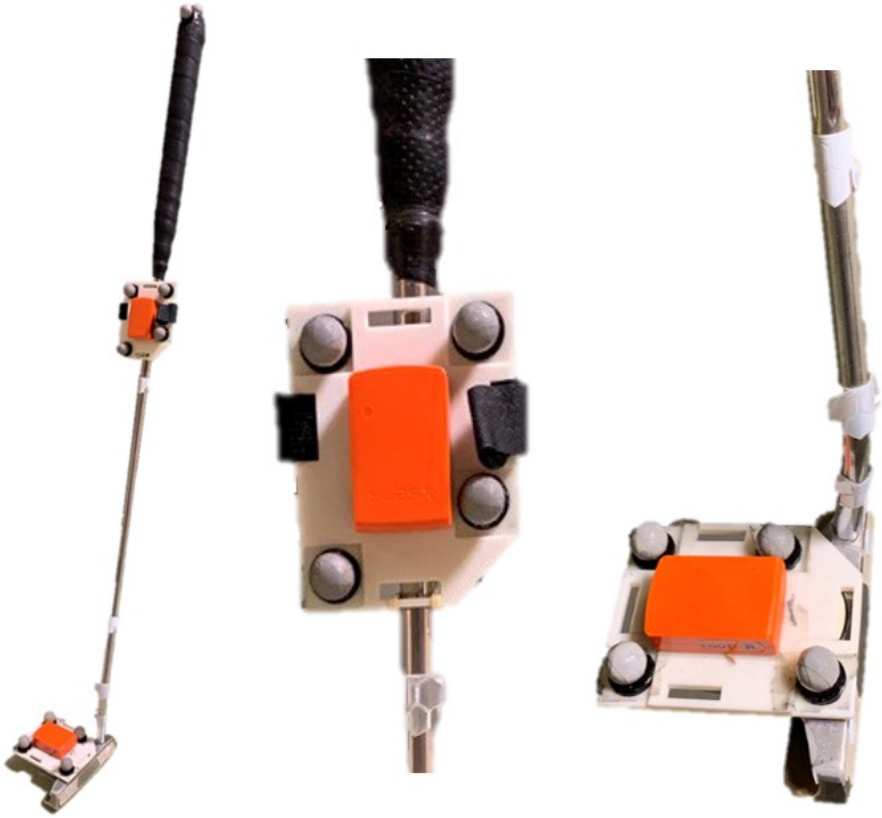

Figure 4.2: Putter equipped with SP markers and IMUs attached to plates.

11.1.1 MTw Performance

	Angular velocity	Acceleration
Dimensions	3 axes	3 axes
Full Scale	± 2000 deg/s	± 160 m/s^2
Non-linearity	0.1 % of FS	0.5 % of FS
Bias stability [11]	10deg/hr	0.1mg
Noise	0.01deg/s/√Hz	200 µg/√Hz
Alignment error	0.1 deg	0.1 deg
Bandwidth	180Hz	180 Hz

Figure 4.3: Performance of IMU Xsens-MTw [46].

In order to fix the IMU sensors on the putter, it was necessary to use plates (Figure 4.2), which provide a stable support surface for the sensors and allow the application of markers visible to SP, which are essential for validating the position of the sensors. The IMU sensors and markers were fixed to the plates with double-sided tape; the plate mounted on the putter head was also attached with double-sided tape, while the one positioned on the shaft, just below the grip, was fastened with Velcro Straps and Elastic Bands. To ensure maximum realism during the trials, a putting practice mat was also employed (Figure 4.4).

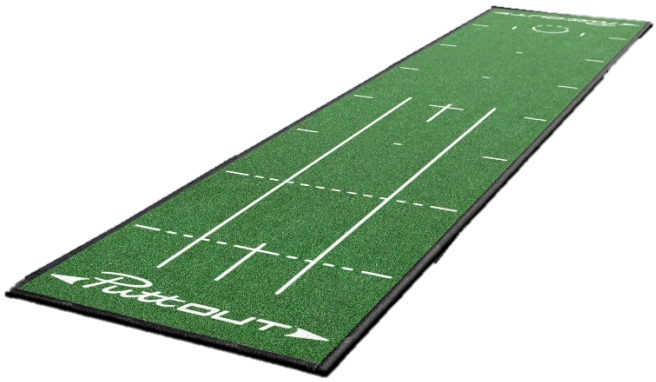

Figure 4. 4: PuttOUT mat for putting practice [47].

4.2 Protocol

The proposed validation protocol involves several preliminary steps to ensure the reliability of the measurements. To mitigate temperature-related effects, an initial sensor warm-up was performed, followed by gyroscope bias calculation and marker preparation. Before experimentation, the SP system was configured through a masking process, full calibration and laboratory reference system setup.

The putter was equipped with optoelectronic markers and IMU sensors, as shown in Figure 4.2, and a static acquisition was performed to allow manual labelling of the markers, ensuring an accurate match with the points detected by the camera system. During the post-processing phases, Nexus software was used to fill in the gaps due to marker occlusion, execute the dynamic pipelines and finally export the data in ASCII format for subsequent analysis.

The study was conducted on a healthy 27-year-old male subject, an amateur golfer, who took 22 strokes to analyse the swing and thus the club trajectory. The shots included several variations to ensure a thorough analysis and to verify that the system was applicable under different conditions and with all types of putting swings.

The trials were captured and analysed with great precision using the combination of the SP and IMU systems, according to the following procedure:

1) 10-minute warm-up of the IMUs;
2) Preliminary acquisition under static 16-marker conditions of five minutes of the IMUs to estimate the gyroscope bias;
3) Starting the acquisition with the IMU software;
4) Start recording with Nexus at 11 markers;
5) Execution of the first shot;

6) Stopping recording with Vicon;
7) Stopping the acquisition of IMUs;
8) Repeat steps 3-7 to acquire additional shots.

During the trial acquisitions, it was necessary to reduce the number of markers from 16 to 11, as some of them were not visible to the infrared cameras for excessively long time intervals.

Once the acquisition procedure is complete, the data recorded by the two inertial sensors and the SP system are saved for further processing. For the IMU, the data are organised in a matrix of size $N_{frame} \times 7$ for each sensor, where the columns represent, in order, the following variables: time series, accelerometer signal along the three axes and gyroscope signal along the three axes. As for the SP, the data are instead stored in a matrix of size $N_{frame} \times (N_{marker} \times 3)$, where the position of each marker is defined along the three directions.

Chapter 5

Results

In this chapter, the results obtained are presented, with a comparison between the proposed optimisation framework and the standard approach discussed above. The SP system was used as the gold standard for data verification. Furthermore, a partial configuration of the optimisation framework will be analysed to highlight the importance of introducing a constraint function in improving the performance of the proposed approach. To this end, three distinct situations were considered:

1. Standard pipeline;
2. Partial optimised pipeline: optimisation limited to two parameters ($\boldsymbol{\beta}, \boldsymbol{b_\omega}$) without the use of a constraint function;
3. Optimised pipeline: optimisation of three parameters ($\boldsymbol{\beta}, \boldsymbol{b_\omega}, \boldsymbol{b_a}$) with the integration of a constraint function.

Finally, a comparison is presented between the results obtained by analysing only the swing phase and those for the entire trial (static and dynamic phases).

5.1 Orientation

Below the results of the orientation estimation are reported, in the dynamic swing phase only, comparing the three methods with the gold standard. The analysis was conducted for each IMU and, in Table 5.1, the mean and standard deviation of the RMSEs obtained in terms of orientation (Equation 5.1) for each trial are presented, evaluating the orientation error angle ($\boldsymbol{\theta_{err}}$) between the estimated ($\boldsymbol{R_{IMU}}$) and

actual ($\boldsymbol{R_{SP}}$) rotation matrix. A comparison of the methods is presented. In addition, a representative example of the proposed optimised pipeline is provided by showing the orientation RMSEs for each sensor in all trials (Figure 5.1).

$$\begin{cases} \theta_{err} = RotMat2AxAng(R_{SP}^{*} \otimes R_{IMU}) \\ RMSE = RMS(\theta_{err}) \end{cases} \tag{5.1}$$

RMSE $[deg]$	Standard Pipeline	Partial Proposed Pipeline	Proposed Pipeline
$mean \pm std$	$1{,}7 \pm 0{,}7$	$1{,}9 \pm 0{,}8$	$1{,}8 \pm 0{,}8$

Table 5. 1: Mean and Standard deviation of the RMSEs obtained in terms of orientation for each trial, with a comparison between the methods.

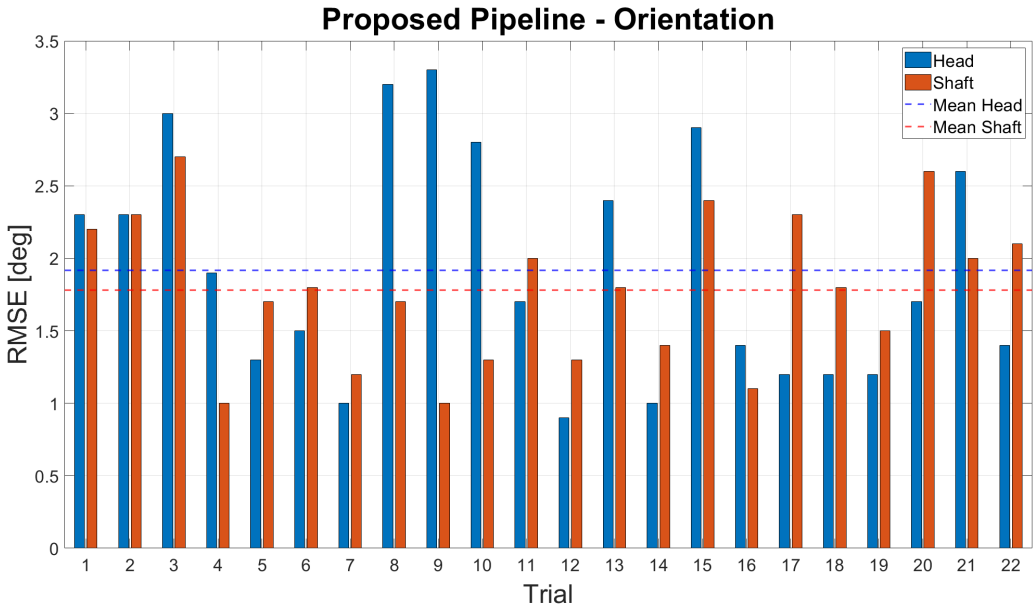

Figure 5. 1: RMSE obtained from the orientation of each IMU for all the trial, analysing the Proposed Pipeline.

5.2 Position

Analogously to Section 5.1, the trajectory comparison is conducted in the swing phase only. The mean and standard deviation of the RMSEs obtained in terms of position (Equation 5.2) for each trial are shown in Table 5.2, evaluating the distance error ($\boldsymbol{d_{err}}$) between the estimated ($\boldsymbol{p_{IMU}}$) and actual ($\boldsymbol{p_{SP}}$) position. A comparison of the different methods for both IMUs is presented.

An example of position RMSE for each sensor across all trials is also shown, compared to the full optimised method (Figure 5.2). Consequently, for both sensors, the position profiles obtained in the various trials were compared (e.g., Figure 5.3). Finally, the difference in the results considering the entire trial versus the swing phase alone was highlighted (Table 5.3), demonstrating the advantages of the proposed method, as will be discussed in Section 6.

$$\begin{cases} d_{err} = \| p_{SP} - p_{IMU} \| \\ RMSE = RMS(d_{err}) \end{cases} \tag{5.2}$$

RMSE $[m]$	Standard Pipeline	Partial Proposed Pipeline	Proposed Pipeline
$mean \pm std$	$0{,}15 \pm 0{,}07$	$0{,}15 \pm 0{,}08$	$0{,}08 \pm 0{,}04$

Table 5. 2: Mean and Standard Deviation of the RMSEs obtained in terms of position for each trial, with a comparison between the methods.

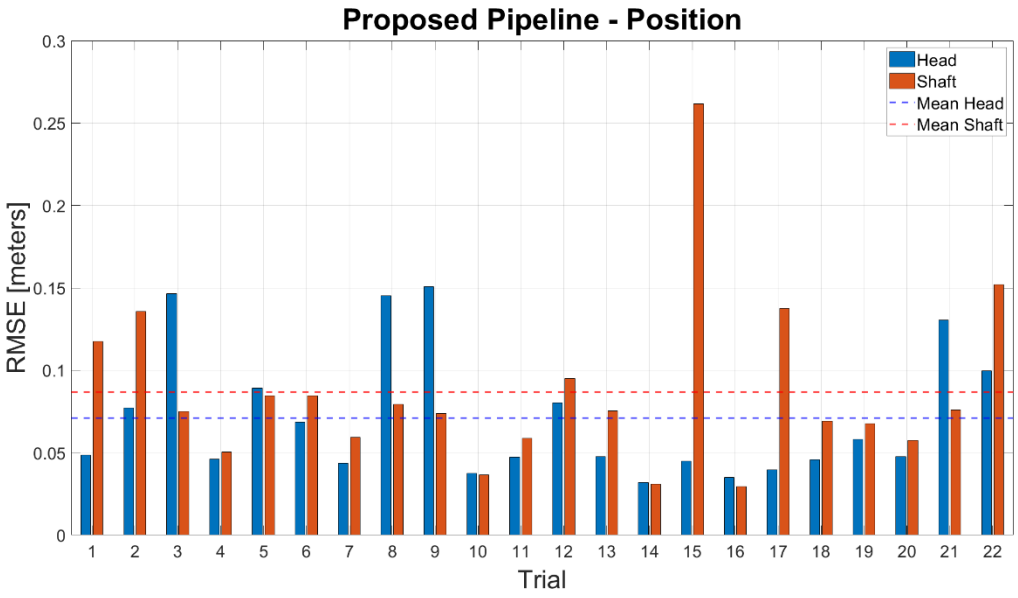

Figure 5. 2: RMSE obtained from the position of each IMU for all the trial, analysing the Proposed Pipeline.

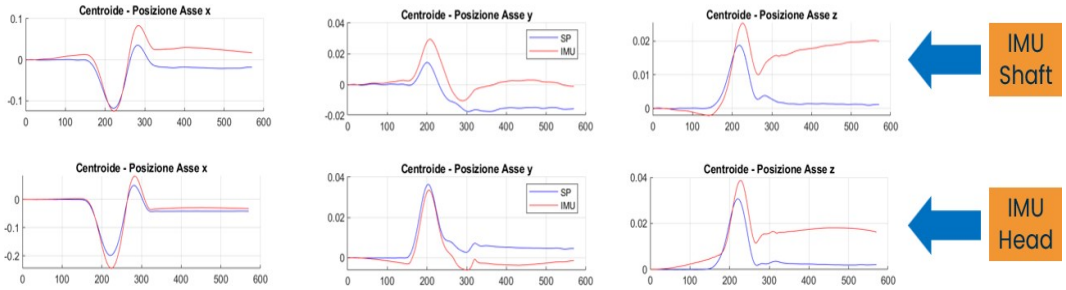

Figure 5. 3: Position profiles obtained from one stroke for both sensors (x-axes [frame], y-axes [meters]).

RMSE $[m]$	Standard Pipeline	Partial Proposed Pipeline	Proposed Pipeline
Swing phase	$0{,}15 \pm 0{,}07$	$0{,}15 \pm 0{,}08$	$0{,}08 \pm 0{,}04$
Trial	$0{,}26 \pm 0{,}19$	$0{,}29 \pm 0{,}17$	$0{,}10 \pm 0{,}06$

Table 5. 3: Differences in terms of RMSE position (mean and standard deviation) between the swing phase and the entire trial.

Chapter 6

Discussion

The aim of this study is to overcome the limitations of current technologies for putt analysis, making it applicable in open field conditions without implementation constraints. The main objective is to evaluate the trajectory of the putter using a redundant configuration with two IMUs, strategically placed on the Shaft and Head of the club. To achieve this, 22 putting strokes were recorded, executed with different techniques to ensure a more comprehensive analysis of possible swing types. A healthy 27-year-old male participant and amateur golfer took the strokes using the putter instrumented with the two IMU sensors and the SP system markers. The data collected from the inertial sensors were integrated into the optimisation framework, together with the results of the first DH model framework. The optimised trajectory was finally compared with that derived from the SP system, in order to evaluate the orientation and position of the sensors during the trials.

6.1 Outcomes and research limitations

As illustrated in Section 5, the results obtained were analysed taking into consideration the orientation and position of the IMUs to assess the potential of the proposed approach.

The first comparison concerns the orientation estimation, which is essential to correctly remove the gravity vector from the accelerometer signal. Table 5.1 shows the average RMSE of the orientation for the dynamic phases of the trials in the three

compared methods. It is observed that the standard method performs slightly better in terms of orientation, as the optimised frameworks mainly aim at reducing position errors, sacrificing part of the accuracy in orientation estimation, as discussed later. Furthermore, Figure 5.1 presents a comparison between the two IMUs for each shot compared to the full optimisation approach. The results demonstrate some variability, alternating between optimal performance and more inaccurate estimation, with performance corrupted more by estimation error. However, it is noticeable that the IMU placed on the Shaft, despite its complex position, offers more stable results.

Regarding position estimation, Table 5.2 shows the average RMSE for the dynamic phases of the trials. As anticipated, the optimised pipeline sacrifices orientation accuracy to improve position estimation. This approach reduces drift errors generated by the integration of residuals into the acceleration vector, demonstrating significantly better performance than the standard method. However, the partial optimisation pipeline shows that relying on only one framework is not sufficient to obtain accurate results, necessitating the introduction of the constraint function to better guide the optimisation process.

A further comparison between the two IMUs for each shot is displayed in Figure 5.2. A correlation can be seen between orientation and position errors: inaccurate orientation estimation negatively affects position, generating drift errors. On average, the IMU positioned on the Head of the putter performs better, with an error of approximately 0.01-0.02 m lower than the Shaft. In many cases, the position error is around 0.05 m, highlighting the potential of the proposed method, which could provide greater reliability and accuracy with further refinement.

Figure 5.3 presents an example of an analysis of sensor position profiles against those recorded by the SP system. The constraints imposed in the optimisation help to correctly estimate known phases, such as stationarity during the static phases, before and after the swing.

Finally, Table 5.3 demonstrates the importance of the constraint function in preventing excessive drift errors, which would otherwise quickly accumulate. The integration of an effective constraint function is crucial to ensure proper parameter optimisation, preventing the accumulation of errors in the acceleration vector and improving the final trajectory estimate.

6.2 Future development

Given that this is a developing method, many aspects presented in this study require further study and evaluation, aimed at improving the performance of the proposed approach. In this sense, as results show, it is important to find other solutions that can mitigate the drifts, mainly caused by the residual accelerometer and gyroscope bias. Consequently, with an eye towards future scientific developments, it may be beneficial to investigate the IMU error model in greater depth, attempting to estimate in detail all the possible errors' contributions recorded by the accelerometer and gyroscope. Indeed, this model could be integrated into the optimization framework in order to obtain a more accurate estimate of these errors. Furthermore, given the low speeds involved, it is very important to thoroughly analyse the accelerometer signal, as any incorrect saturation points or readings are unlikely to occur: instead, the signal may be minimally affected by the vibrations deriving from the impact with the bat.

Another important aspect to concentrate on to enhance the method's performance relies on focusing on the constraint function, to introduce new constraints aimed at facilitating the optimization in finding feasible solutions. However, this would generate an high computational load: in fact, introducing too many parameters to optimise and boundary conditions to the constraint function would require a too long processing time, while the method proposed in this study necessitates about 5 minutes per trial.

Finally, many other elements can be introduced, either to help the optimization to better navigate the solution space, or to provide a more detailed analysis. For instance, an investigation into the correlation between the swing and the shot taken may be carried out, to propose an estimation of the ball's trajectory as a consequence of the data at impact. Furthermore, by integrating an additional IMU sensor into the golf glove it would be possible to determine a correlation between the golfer's biomechanics and the putter trajectory.

Lastly, it would be critical to expand the dataset by acquiring additional trials from various players. This would enrich the information available, enabling a more comprehensive evaluation of different swing possibilities, while also facilitating the implementation of boundary conditions.

Chapter 7

Conclusion

Golf stands out as a sport where the precision and repeatability of the technical gesture are fundamental elements for enhancing performance. For this reason, given the complexity of this sport, it is essential to be able to train in a targeted manner. In this sense, a significant golf limitation consists in the need to analyze the technical gesture exclusively in dedicated spaces, such as simulators or practice ranges, making it difficult to carry out evaluations in the open field during a game. This research aims to propose an innovative solution for open-field monitoring of the putting stroke, the most frequent and decisive shot in tournaments. Emerging technologies, such as wearable devices and sensory fusion techniques, offer promising alternatives, laying the basis for feasible solutions for a more effective and accessible analysis.

In the present study, an innovative method was developed to perform this analysis. By implementing a minimal redundant configuration of inertial sensors, the putter was modelled following the DH convention, integrated into an optimization framework. This approach permits to estimate the orientation and position of the putter and evaluate its performance through the SP system. The results obtained, measured in terms of RMSE, showed good accuracy in orientation. However, significant limitations still emerge in the estimation of position, which do not yet achieve the necessary level of precision required for a complete and accurate analysis of the technical gesture. Therefore, in the future scientific field it will be

crucial to find solutions to reduce the errors introduced by IMU signals, in order to limit the accumulative drifts in position estimation.

Despite these limitations, this study has demonstrated the potential of the proposed approach for analyzing open-field putting, opening up new perspectives for the application of similar technologies to other shots in golf and even other sports

Bibliography

[1] Wiley Online Library, "Introduction to Biomechanics," [Online]. Available: https://onlinelibrary.wiley.com/doi/book/10.1002/9780470713174#page=313. [Accessed: Feb. 25, 2024].

[2] Match Collegiate, "Opinion: Golf is the Most Difficult Sport," [Online]. Available: https://www.matchcollegiate.org/2023/03/27/opinion-golf-is-the-most-difficult-sport/. [Accessed: Mar. 2, 2024].

[3] Universiti Teknologi MARA Institutional Repository, "Research Repository," [Online]. Available: https://ir.uitm.edu.my/id/eprint/22088/. [Accessed: Mar. 10, 2024].

[4] PGA Tour, "Putting Statistics," [Online]. Available: www.pgatour.com/stats/putting. [Accessed: Feb. 22, 2024].

[5] T. Stickney II, "Lag Putting: Why You're Doing It Wrong," Golf WRX, Mar. 26, 2022. [Online]. Available: www.golfwrx.com/673601/stickney-lag-putting-why-youre-doing-it-wrong/. [Accessed: Mar. 27, 2024].

[6] Science and Motion, "SAM PuttLab," [Online]. Available: https://www.scienceandmotion.com/puttlab/. [Accessed: Mar. 12, 2024].

[7] Quintic Sports, "Quintic Ball Roll," [Online]. Available: https://www.quinticsports.com/quintic-ball-roll/. [Accessed: Mar. 12, 2024].

[8] Trackman, "Golf Simulator," [Online]. Available: www.trackman.com/golf/simulator. [Accessed: Mar. 27, 2024].

[9] U. Jensen, et al., "An IMU-based mobile system for golf putt analysis," *Sports Engineering*, vol. 18, pp. 123–133, 2015.

[10] M. S. Couceiro, A. G. Araújo, and S. C. Pereira, "InPutter: an engineered putter for on-the-fly golf putting analysis," *Sports Technology*, vol. 8, no. 1–2, pp. 12–29, 2015.

[11] G. Dias, et al., "Golf-Putting Performance in Skilled Golfers at Different Distances to the Hole," *Applied Sciences*, vol. 11, no. 24, p. 11785, 2021.

[12] H. Kawano, et al., "Design and Basic Experiment of Online Feedback Training System for Golf Putting," in *Proc. IEEE/SICE Int. Symp. System Integration (SII)*, 2021, pp. 1–5.

[13] Jag Putters, "Lie, Loft, Length, Offset," [Online]. Available: http://www.jagputters.com/en/about-putters/lie-loft-lenght-offset/. [Accessed: Sept. 14, 2024].

[14] D. J. Kooyman, D. A. James, and D. D. Rowlands, "A feedback system for the motor learning of skills in golf," *Procedia Engineering*, vol. 60, pp. 226–231, 2013.

[15] U. Jensen, et al., "Sensor-based instant golf putt feedback," in *Proc. IACSS*, 2011, pp. 49–53.

[16] R. Burchfield and S. Venkatesan, "A framework for golf training using low-cost inertial sensors," in *Proc. Int. Conf. Body Sensor Networks*, 2010, pp. 77–83.

[17] K. King, et al., "Wireless MEMS inertial sensor system for golf swing dynamics," *Sensors and Actuators A: Physical*, vol. 141, no. 2, pp. 619–630, 2008.

[18] S. Buhl and U. Böller, "Golf Indoor: Putting Technique," *Mobile Sport*, Nov. 10, 2020. [Online]. Available: https://assets01.sdd1.ch/assets/lbwp-cdn/mobilesport/files/1604995209/mt_11_20_golf_indoor_d.pdf. [Accessed: Sept. 29, 2024].

[19] A. Cereatti, D. Trojaniello, and U. Della Croce, "Accurately measuring human movement using magneto-inertial sensors: techniques and challenges," in *Proc. IEEE Int. Symp. Inertial Sensors and Systems (INERTIAL)*, 2015, pp. 1–5.

[20] E. Bergamini, et al., "Estimating orientation using magnetic and inertial sensors and different sensor fusion approaches: Accuracy assessment in manual and locomotion tasks," *Sensors*, vol. 14, no. 10, pp. 18625–18649, 2014.

[21] S. Madgwick, "An efficient orientation filter for inertial and inertial/magnetic sensor arrays," *University of Bristol Report*, vol. 25, pp. 113–118, 2010.

[22] G. A. Aydemir and A. Saranlı, "Characterization and calibration of MEMS inertial sensors for state and parameter estimation applications," *Measurement*, vol. 45, no. 5, pp. 1210–1225, 2012.

[23] D. Unsal and K. Demirbas, "Estimation of deterministic and stochastic IMU error parameters," in *Proc. IEEE/ION Position, Location and Navigation Symp.*, 2012, pp. 327–331.

[24] A. Nez, et al., "Comparison of calibration methods for accelerometers used in human motion analysis," *Medical Engineering & Physics*, vol. 38, no. 11, pp. 1289–1299, 2016.

[25] G. Aslan and A. Saranli, "Characterization and calibration of MEMS inertial measurement units," in *Proc. 16th European Signal Processing Conf.*, 2008, pp. 1447–1451.

[26] M. Kirkko-Jaakkola, J. Collin, and J. Takala, "Bias prediction for MEMS gyroscopes," *IEEE Sensors Journal*, vol. 12, no. 6, pp. 2157–2163, 2012.

[27] F. Ferraris, U. Grimaldi, and M. Parvis, "Procedure for effortless in-field calibration of three-axial rate gyro and accelerometers," *Sensors and Materials*, vol. 7, no. 5, pp. 311–330, 1995.

[28] M. Caruso, et al., "Analysis of the accuracy of ten algorithms for orientation estimation using inertial and magnetic sensing under optimal conditions: One size does not fit all," *Sensors*, vol. 21, no. 7, p. 2543, 2021.

[29] F. Gulmammadov, "Analysis, modeling and compensation of bias drift in MEMS inertial sensors," in *Proc. 4th Int. Conf. Recent Advances in Space Technologies*, IEEE, 2009, pp. 389–394.

[30] T. Hiller, et al., "Origins and mechanisms of bias instability noise in a three-axis mode-matched MEMS gyroscope," *Journal of Microelectromechanical Systems*, vol. 28, no. 4, pp. 586–596, 2019.

[31] A. Walther, et al., "Bias contributions in a MEMS tuning fork gyroscope," *Journal of Microelectromechanical Systems*, vol. 22, no. 2, pp. 303–308, 2012.

[32] S. O. H. Madgwick, A. J. L. Harrison, and R. Vaidyanathan, "Estimation of IMU and MARG orientation using a gradient descent algorithm," in *Proc. IEEE Int. Conf. Rehabilitation Robotics*, IEEE, 2011, pp. 1–7.

[33] K. Lebel, P. Boissy, M. Hamel, and C. Duval, "Inertial measures of motion for clinical biomechanics: comparative assessment of accuracy under controlled conditions—effect of velocity," *PLoS One*, vol. 8, no. 11, pp. 1–14, Nov. 2013.

[34] K. Lebel, P. Boissy, M. Hamel, and C. Duval, "Inertial measures of motion for clinical biomechanics: comparative assessment of accuracy under controlled conditions—changes in accuracy over time," *PLoS One*, vol. 10, no. 3, pp. 1–14, Mar. 2015.

[35] S. A. Ludwig and K. D. Burnham, "Comparison of Euler Estimate using Extended Kalman Filter, Madgwick and Mahony on Quadcopter Flight Data,"

in *Proc. 2018 Int. Conf. Unmanned Aircraft Systems (ICUAS)*, Dallas, TX, USA, Jun. 2018, pp. 1236–1241.

[36] M. Nazarahari and H. Rouhani, "40 years of sensor fusion for orientation tracking via magnetic and inertial measurement units: Methods, lessons learned, and future challenges," *Information Fusion*, vol. 68, pp. 67–84, Apr. 2021.

[37] L. Ricci, F. Taffoni, and D. Formica, "On the Orientation Error of IMU: Investigating Static and Dynamic Accuracy Targeting Human Motion," *PLoS One*, vol. 11, no. 9, pp. 1–14, Sept. 2016.

[38] D. Weber, C. Gühmann, and T. Seel, "Neural Networks Versus Conventional Filters for Inertial-Sensor-based Attitude Estimation," in *Proc. 2020 IEEE Int. Conf. Information Fusion (FUSION)*, Rustenburg, South Africa, Jul. 2020, pp. 1–8.

[39] A. D. Young, "Comparison of Orientation Filter Algorithms for Real-Time Wireless Inertial Posture Tracking," in *Proc. 6th Int. Workshop Wearable and Implantable Body Sensor Networks*, Berkeley, CA, USA, Jun. 2009, pp. 59–64.

[40] A. Cavallo, et al., "Experimental Comparison of Sensor Fusion Algorithms for Attitude Estimation," in *IFAC Proc. Volumes*, vol. 47, no. 3, pp. 7585–7591, 2014.

[41] M. Caruso, "Methods and good practice guidelines for human joint kinematics estimation through magnetic and inertial wearable sensors," Ph.D. dissertation, Politecnico di Torino, Italy, 2022.

[42] A. Olivares, J. M. Górriz, J. Ramírez, and G. Olivares, "Using frequency analysis to improve the precision of human body posture algorithms based on Kalman filters," *Computers in Biology and Medicine*, vol. 72, pp. 229–238, May 2016.

[43] B. Siciliano, L. Sciavicco, L. Villani, and G. Oriolo, *Robotics - Modelling, Planning and Control*, London, U.K.: Springer, 2009, pp. 14–15.

[44] Wikipedia contributors, "Sequential quadratic programming," *Wikipedia, The Free Encyclopedia*, [Online]. Available: https://en.wikipedia.org/wiki/Sequential_quadratic_programming. [Accessed: Apr. 13, 2023].

[45] J. Nocedal and S. J. Wright, *Numerical Optimization*, 2nd ed. New York, NY, USA: Springer, 2006.

[46] Xsens, *MTw Awinda User Manual*, [Online]. Available: https://www.xsens.com/hubfs/Downloads/Manuals/MTw_Awinda_User_Manual.pdf. [Accessed: Apr. 7, 2024].

[47] PuttOUT, "Medium Putting Mat," [Online]. Available: https://puttout.golf/products/medium-putting-mat. [Accessed: Mar. 24, 2024].

[48] M. Caruso, et al., "Magnetic and inertial sensor data fusion for orientation estimation," *IEEE Sensors Journal*, vol. 21, no. 3, pp. 3408–3419, 2020.